

Research of the Voltage Stability of Distribution Network Connected Induction Machines

Trinh Trong Chuong¹, Traong Viet Anh², Tran Quang Tho², Tomas Deveikis³

¹Hanoi University of Industry,
Hanoi, Vietnam

²University of Technical Education,
Hochiminh City, Vietnam

³Department of Electrical Power Systems, Kaunas University of Technology,
Studentu St. 48, LT-51367 Kaunas, Lithuania
tomas.deveikis@ktu.lt

Abstract—There are a lot of wind power plants based on double feed induction machine technology which are connected to electrical network. These usually don't consider reactive power (even reactive power consumption), so they generally affect the entire network voltage stability and can cause instability in themselves and become no longer balanced by the torque. This paper presents a method to study the relationship between the active power and voltage at the point of common coupling (PCC) connected wind power plant to identify the voltage stability limit. It is a fundament to define a permitted operation region in complying with the voltage stability limit at the PCC connected wind power.

Index Terms—DFIM, PCC, PV curve, Thevenin, voltage stability.

I. INTRODUCTION

In distribution networks without distributed generation using induction machine (IM), voltage instability may occur when increasing load power or changing operating conditions. The main factor causing voltage instability is corresponding inability of demand reactive power in the distribution network. The parameters related to voltage collapse are the active power and reactive power of the network. When distributed generators (DG) are connected to the network, this problem becomes more complex because DG has many potential factors causing voltage instability. If DG is induction machine, then it does not supply the reactive power, so DG can affect overall stability of voltage of the network, and can cause instability in itself by no longer balance work torque [1]. This is the case of wind power connection with induction machine in the distribution networks. Therefore, the study of voltage stability in the distribution networks relative to DG aims to understand the structure causing voltage instability, and reliability analysis of work stability (sufficient reserve stability coefficients) of DG itself.

This paper studies the factors to ensure voltage stability for induction machine of the wind turbine working in distribution networks. First of all, distribution network with induction machine is modelled, and then voltage stability

analysis tool is built in terminal connection of induction machine.

II. MODELLING OF INDUCTION MACHINE IN WIND TURBINES

A. Model of Squirrel Cage IM in Wind Turbines

Equivalent diagram of induction machine is shown in Fig. 1. The relationship between the slip and the torque is shown in Fig. 2 [2].

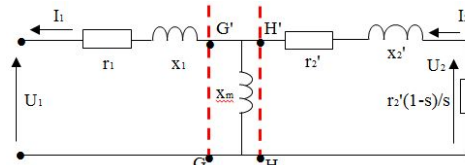


Fig. 1. The equivalent circuit of induction machine.

In the equivalent circuit, the load is replaced by a resistance $r_2(1-s)/s$. Dissipation energy in the resistance is equivalent to electrical energy converted into mechanical energy on drive shaft when IM rotates. In the induction machine, due to small magnetizing current, magnetizing reactance x_m is unchanged (ignoring resistance r_m), the loss of motor doesn't include iron loss.

In Fig. 1, U_1 and I_1 are the voltage and current of the stator; U_2 and I_2 are the voltage and current of rotor; r_1 and x_1 are the resistance and reactance of the stator winding; r_2' and x_2' are resistance and reactance of the rotor circuit. From the equivalent circuit in Fig.1 [2]:

$$R(s) = \frac{x_m^2 \times \frac{r_2'}{s}}{\left(\frac{r_1'}{s}\right) + (x_m + x_2')^2}, \quad (1)$$

$$X(s) = \frac{x_m^2 \times x_2' + x_m \times x_2'^2 + x_m \left(\frac{r_2'}{s}\right)^2}{\left(\frac{r_1'}{s}\right)^2 + (x_m + x_2')^2}. \quad (2)$$

Combined with the impedance of stator, it will calculate the power of generator [2]:

$$P_e(U, s) = \frac{-[r_1 + R(s)] \times U^2}{[r_1 + R(s)]^2 + [x_1 + X(s)]^2}, \quad (3)$$

$$Q_e(U, s) = \frac{-[x_1 + X(s)] \times U^2}{[r_1 + R(s)]^2 + [x_1 + X(s)]^2}. \quad (4)$$

The above equations show that: the capacity of the power depends mainly on two parameters: the slip and terminal voltage [3], [4]. Further torque characteristic of the generator in this case is the same with induction motors. Specifically, in Fig. 2, if the power is reversed (positive with generation capacity) and calculating the slip (s), it will have the characteristics completely the same with the characteristics of motor, the formulas do not change

$$s = [(\tilde{S} - \tilde{S}_0) / \tilde{S}_0], \quad (5)$$

where s is the slip, ω is the angular speed of rotor, ω_0 is the angular speed of the stator.

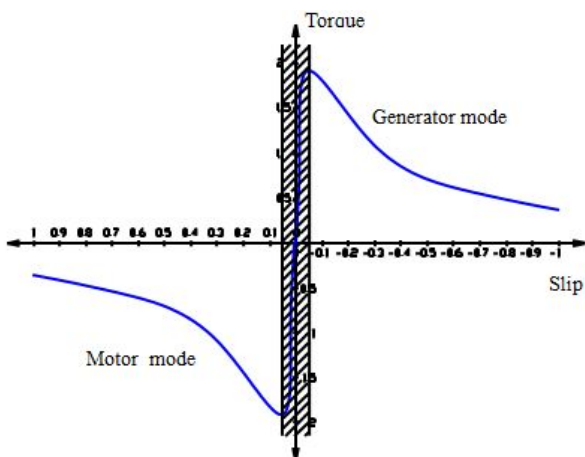


Fig. 2. Torque of squirrel cage induction machine as a function of slip.

B. Model of Induction Machine Dual Power Type in Wind Turbine (DFIM)

DFIM can supply power from the rotor to the network (through power converters) and stator (Fig. 3). This converter allows DFIM work in all four quadrants of the complex plane, it means that DFIM has ability to supply reactive power Q to the network. Reactive power which is exchanged between network and DFIM can be controlled independently on the real power. In DFIM, the magnitude of the torque shows the magnitude of generating power and motoring power in Fig. 4.

Total active power to the network of DFIM is power of the rotor ($P_r = -sP_s$) and stator's (P_s) of the generator [5]

$$P_{DFIM} = P_s + P_r = (1-s) \times P_s. \quad (6)$$

Distribution of power between the stator and rotor windings of DFIM depends on the slip. Power through the rotor circuit opposites and approximately equals to the product of the stator coil power and the slip. Depending on

operating conditions, the power in rotor circuit can follow in both directions: from the network through power converters to the rotor, $P_r < 0$, under the synchronous mode (Fig. 4(b)) and from the rotor circuit through the inverter to power networks, $P_r > 0$, upper the synchronous mode (Fig. 4(c)). In both cases, stator circuit still supplies power to the network, $P_s > 0$. Total reactive power that the generator supplies to the network will be the sum of the stator reactive power and reactive power network side converter. This generator type has very large magnetizing reactance, so it can be considered equivalent diagram in Fig. 3 the same with Fig. 5. In this figure, the generator stator voltage is $U_1 \angle 0$ and the generator rotor voltage is $U_r/s \angle \delta$.

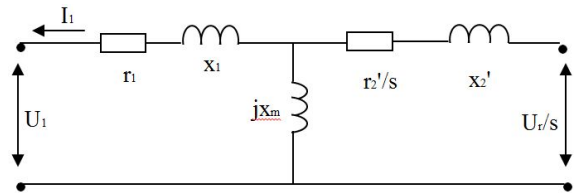


Fig. 3. The equivalent circuit of DFIM.

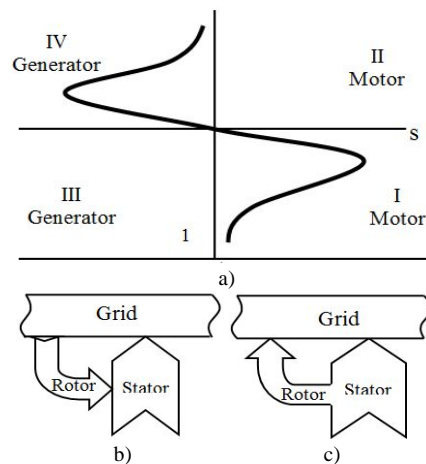


Fig. 4. Torque-slip characteristics DFIM (a), flow currents from distribution grid when DFIM starts (b), and flow current when DFIM works like DFIG (c).

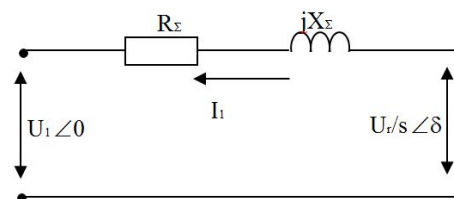


Fig. 5. Simplified diagram of DFIM.

From the diagram, it is easily to calculate the stator output power: $P_s = \text{Re}[U_1 \cdot I_1^*]$. Specifically

$$P_s = - \frac{\left[X_\Sigma(s) \times \frac{U_r}{s} \times \sin u - R_\Sigma(s) \left(U_1 - \frac{U_r}{s} \times \cos u \right) \right]}{R_\Sigma^2(s) + X_\Sigma^2(s)} \times U_1, \quad (7)$$

where R_Σ and X_Σ are respectively resistance and equivalent resistance of DFIM.

Ignoring resistors of generator, (7) becomes

$$P_s = - \left(U_1 \frac{U_r}{s} \times \sin u \right) / X_\Sigma(s). \quad (8)$$

When angle δ changes, the stator active power P_s (8) depends on slip s and DFIM can be analysed for synchronous and asynchronous rotating speed conditions. Nowadays, with modern control technology, the generators are usually adjusted to generate power to the network through the stator circuit or operate in constant power factor [6]–[8].

III. VOLTAGE STABILITY IN CONNECTION BUS WITH DG

There are 2 scenarios to determine the voltage stability limit in distribution network connected induction machine:

- Firstly: Due to load capacity growth, while the amount of reactive power load exceeds the limit of the network;
- Secondly: When they are connected on the network, then there will be the high risk of voltage instabilities due to strong influence of reactive power.

This content refers to the later scene. From the static model of induction machine as shown in Fig. 6, after solving the problem power flow, active and reactive powers of DG are completely determined. DG voltage stability depends only on the parameters of the terminal voltage. So, it can change the form of diagram Fig. 6(a) to the simple diagram (Fig. 6(b)). As shown in Fig. 6(b), the equation for power at node T is represented as (9) [4] and [9]

$$\frac{-AU_T^2}{B} \angle s - r + \frac{U_{HT} \times U_T}{B} \angle (s - u) = P_T + jQ_T, \quad (9)$$

where A, B are equivalent constants of the network.

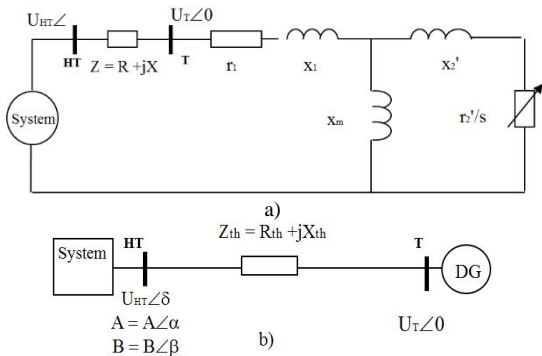


Fig. 6. Diagram of distribution network power connection to DG (a) and the equivalent model (b).

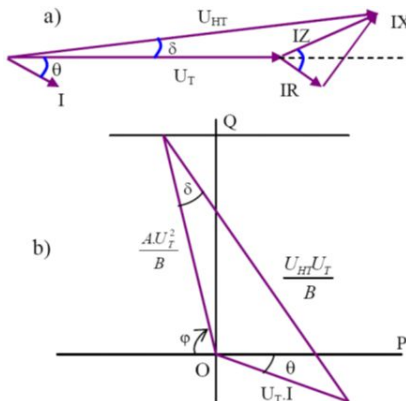


Fig. 7. Phasor diagram of DFIM.

If the values of phasors (Fig. 7(a)) are multiplied by U_T/B and the diagram (Fig 7(a)) is rotated according to the angle θ around the base, the new diagram corresponding to (9) can

be created (Fig. 7(b)). Next, a straight line KC' should be drawn so that $OC'K$ angle equals OKC angle (angle ζ in Fig. 8). Angle between KC' and KO straight lines is angle δ' . The intersections and phase angle ϕ' are shown in Fig. 8.

Having $\zeta' = 180^\circ - (s - r) + \dots$ and $u' = u - r$. From the Fig. 8:

$$\begin{cases} OC = \frac{AU_T^2}{B}, \\ OK = S_T, \\ CK = \frac{U_T U_{HT}}{B}. \end{cases} \quad (10)$$

Application of the OCK triangular relation

$$\frac{OK}{\sin u'} = \frac{CK}{\sin \zeta'} = \frac{OC}{\sin \zeta}. \quad (11)$$

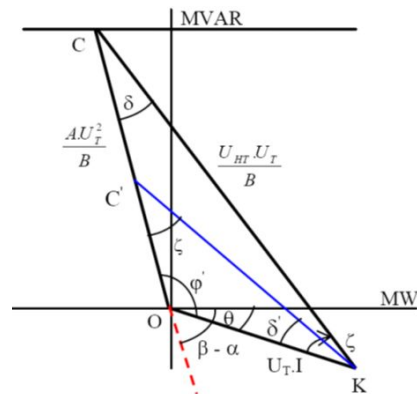


Fig. 8. Vector diagram on the PQ complex power plane.

From (11), S_T is calculated as

$$S_T = \frac{A \cdot U_T^2 \times \sin u'}{B \times \sin \zeta} = \frac{U_T U_{HT} \times \sin u'}{B \times \sin \zeta}, \quad (12)$$

so

$$U_T = \frac{U_{HT} \times \sin \zeta}{A \sin \zeta'}. \quad (13)$$

To replace U_T in (13) to (12)

$$S_T = \frac{U_{HT}^2 \times \sin \zeta \times \sin u'}{AB \times \sin^2 \zeta'}. \quad (14)$$

S_T value is reached limit

$$\frac{dS_T}{du} = \frac{dS_T}{du'} = \frac{U_{HT}^2}{AB} \times \frac{\sin(s - r + u' - 2u)}{\sin^2(s - r - u')} = 0. \quad (15)$$

So $u_{gh} = 1/2(s + r - r)$ and $u_{gh}' = u_{gh} - r$. To replace this value to (14)

$$S_{T-th} = \frac{U_N^2 \sin^2 [(1/2)(s - r - r)]}{AB \times \sin^2 (s - r - r)}. \quad (16)$$

To replace $\gamma' = [180^\circ - (s - r) + \dots]$ to (16)

$$S_{T-gh} = \frac{U_{HT}^2}{4AB \cdot \sin^2 \{\gamma/2\}} \quad (17)$$

To replace $u = u_{th} = 1/2(s + r - \dots)$ to (13), through a number of changes obtained

$$U_{T-gh} = \frac{U_{HT}}{2A \times \sin \{\gamma/2\}} \quad (18)$$

From (12) to (18) showing

$$S_T = \frac{S_{T-th} \left[\sin(\{\gamma' + u'\}) \sin u' \right]}{\cos^2 \{\gamma/2\}} \quad (19)$$

The voltage at connection node

$$U_T = \frac{U_{HT} \times \sin(\{\gamma' + u'\})}{A \times \sin \{\gamma'\}} \quad (20)$$

The derived expressions allow to evaluate dependence of limit values of voltage and power P_{gh} on the angle θ at the node, Thevenin impedance and connection node voltage. If power factor of node T is small then P_{gh} decreases. If the power factor remains constant while increasing the power of DG to the node, it will cause voltage drops, to a certain limit it will not exist stability mode. The advantage of this tool is able to find the limit values, not to aggravate or solve solutions of biquadratic equations.

When DG changes the power, the determination of the limited parameters is not complex. The values of voltage and power (19) and (20) compose the pair values on the boundary of above and below the PV curve. The model determines the limit of the voltage stability of the DG showing in Fig. 9.

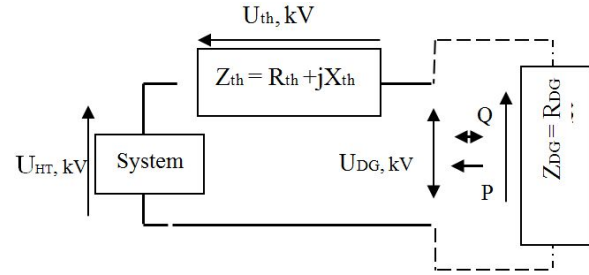


Fig. 9. The survey model of node voltage stability limit mode of the distribution network with DG.

Specifically, construction of PV curves as follows:

- To enter the network and connected node;
- To identify the equivalent constant of the power network [A, B, C, D] and the values of α, β ;
- To identify slip and reactive power of the DG;
- From step 3, determine the power factor at DG connection node and the power limit values and the voltage at node;
- To determine $u' = u_{gh} \pm \Delta u$ with $u_{gh} = 1/2 \times (s + r - \dots)$ and to change Δu (in degree);
- To calculate S_T, U_T and to draw the PV curve.

IV. COMPUTING APPLICATION

Ninh Thuan regional network by 2015 (Fig. 10) in Vietnam is going to have connection of wind power farm (WP) are 20 MW of network connected at 22 kV [3].

As in Fig. 11, the wind power generators will be connected to the node 99 to inject into the power system. Voltage of the node 100 equals to 22 kV which corresponds to the high voltage of the transformer 0,69/22 kV of wind generators. Due to power generators, including many of the same parameters, so the results of this calculation determine voltage stability limit for each unit when connecting to the network. The fact that these values changing step by step, but it is assumed to be constant to analyse the limit mode.

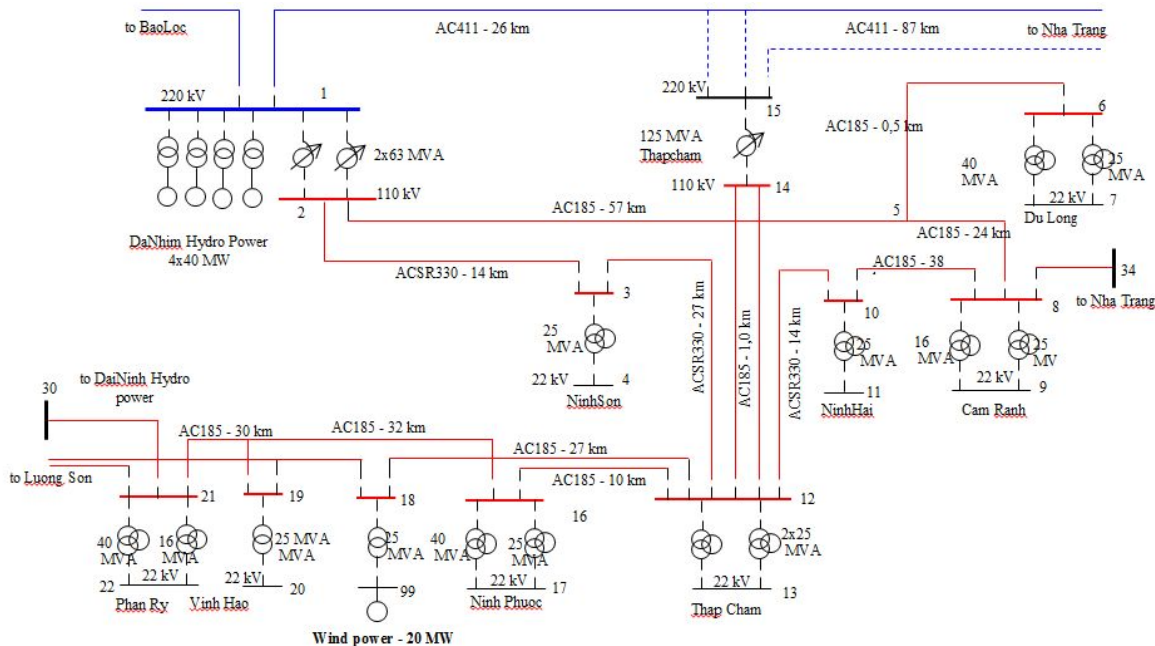


Fig. 10. Diagram of Ninh Thuan network connected 20 MW wind power by 2015.

Calculated results are set out with two types of generators: induction machine with squirrel cage rotor and DFIM. In addition, the solutions: putting compensated capacitors, network reconfiguration, using transformer adjusted under load are also considered to compare the efficiency of the voltage stability of the network in Ninh Phuoc by 2015.

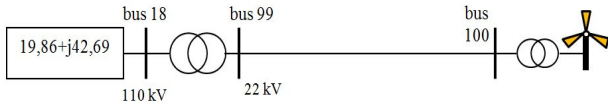


Fig. 11. Simplified computational scheme of electrical network with connected WP.

The system impedance connected to node is $Z = 0.16414 + j0.35281$ (node 18 in Fig. 11) in the per unit system ($S_{cb} = 100$ MVA) (issued by the National load dispatch centre of Vietnam – NLDC).

To determine the limit values, firstly, we need to solve power flow to find initial conditions [1]. After getting the data values, P , Q and s of generator which completely determined at a point on the power curve, as it will apply the method to build PV curve in Section A to draw the stability curve.

A. Analysis of Voltage Stability at Nodes Connected WP with IM Generator

In the first mode, DG generates active power and receives reactive power, the power factor angle is defined as: $\theta = \arctan(Q/P) = -0.670^\circ$ (lag) [4]. The results showed that in the basic operating modes, when Ninh Phuoc wind power generates active power and receives reactive power. P_{gh} – the limited power at connected node reaches 20.72 MW and U_{gh} – the limited voltage is 0.68 pu (Table I).

TABLE I. LIMITED NUMBERS OF CONNECTED NODE AS OPERATING NATURAL MODE OF IM.

α , degrees	β , degrees	S_{Tgh} , MVA	P_{Tgh} , MW	Q_{Tgh} , MVAR	U_{gh} , degrees	U_{Tg} , pu
0.67	117.3	20.72	20.71	0.24	31.3	0.68

To improve the power and voltage limits, we can propose a number of solutions such as putting capacitors, reconfiguring area with wind turbines, or using on load tap changer (OLTC) for power transformers and the 5 MVAR of compensated capacitor is connected the node. The aggregate results of the proposed methods mentioned above are showed in Fig. 12.

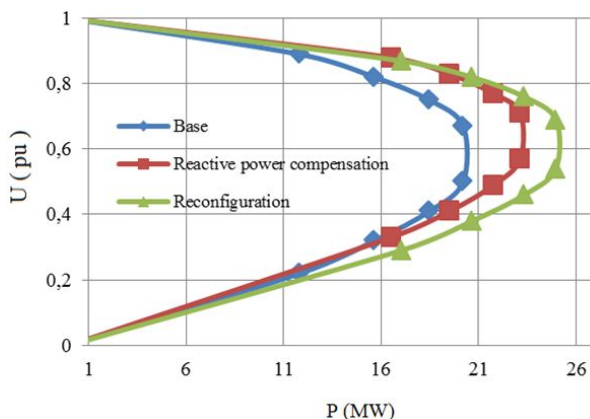


Fig. 12. Results of computation schemes at WP Ninh Thuan connected node (IM).

It is easy to show that placing compensated capacitors and using OLTC improve the operating voltage better, however, they make voltage drop larger due to operation voltage near U_{gh}. Using reconfigured network has better results, Power P_{gh} increased to 25.5 MW (23.2 % increasing). This result also shows that reconfiguration of the network not only reduces power loss, but also significantly improves stability voltage when the network is having induction machine.

B. Analysis of Voltage Stability at Nodes Connected WP with DFIM Generators

With the given parameters [4], after finding the initial conditions, we apply the formula (6): PDFIM = P_{stato} + sP_{stato} = 2.0005 MW. It follows that: $Q = \text{Im}[U111] = 0.33$ MVAR and $\theta = 9.3^\circ$ (lead). The results of the calculations limited values are given in Table II.

TABLE II. LIMITED NUMBERS OF CONNECTED NODE OF DFIM.

α , degrees	β , degrees	S_{Tgh} , MVA	P_{Tgh} , MW	Q_{Tgh} , MVAR	U_{gh} , degrees	U_{Tg} , pu
9.3	107.4	22.85	22.55	3.69	36.3	0.69

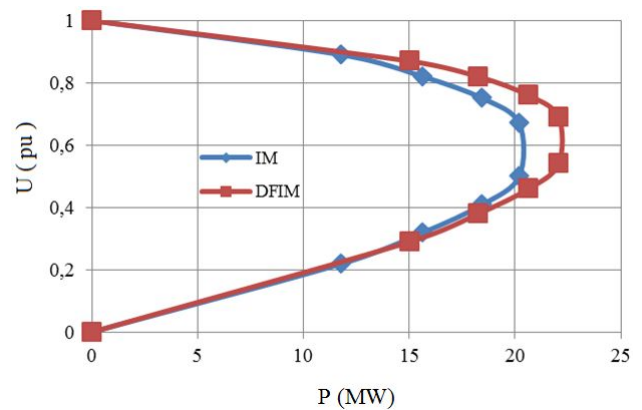


Fig. 13. PV curves between IM and DFIM.

Comparing with the use of IM in Table II and Fig. 13 shows that as the same value of output power, DFIM has got better voltage quality. In addition, limited power at connected node increased by 9 % compared to the use of IM. The limited power reached 22.55 MW and limited voltage is 0.69 pu. Method of reconfiguration the WP region network has good results in PV characteristic format in Fig. 14.

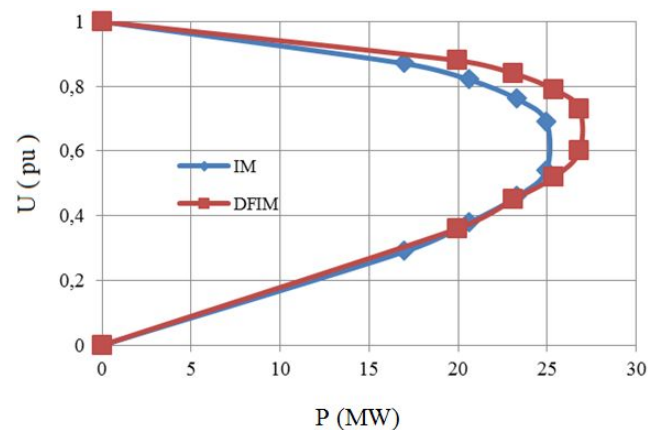


Fig. 14. PV curves after reconfiguration.

Voltage at connected DFIM node is down to 0.88 pu. Resolving the power flow, because the power of WP will decline by WP's power depends on U and s . Found result

$P_{stato} = 1.178$ MW, inferred PDFIM = $P_{stato} + P_{proto} = 1.337$ MW and $Q = -0.18$ MVAR. Then calculated $\theta = \arctan(Q/P) = -7.7$ (lag phase). And then $\varphi' = [180 - (\beta - \alpha) + \theta] = 109.3^\circ$. Calculated results are shown in Fig. 15.

When the voltage of connecting node reduces, it causes the slip increase, the voltage at this node decrease and the amount of reactive power which receives from the network greater, the process leads to faster voltage instability proceeds, P_{gh} power declined dramatically.

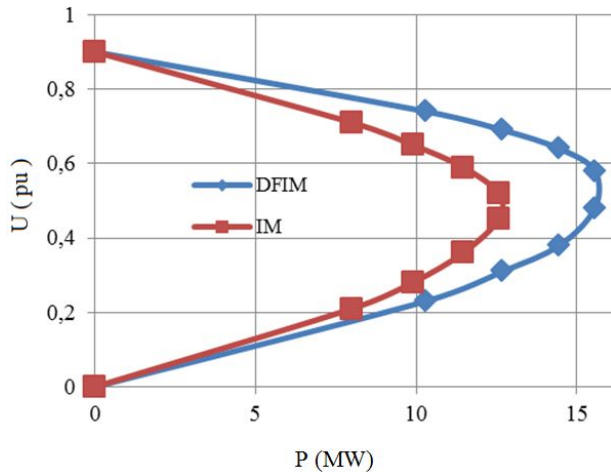


Fig. 15. PV curves at connected DFIM and IM node when the voltage decline.

Due to low output power of the wind generators connected to the distribution network reduces sharply the voltage of network when the network is outage from the fault. With the decline of the threshold voltage to less than 90 % of nominal voltage, in the time of 100 ms, the generator will have to be cut out of the regular network whenever a fault near the connection node happens.

As mentioned problems above, most electricity companies require the wind power generators to cut out when the voltage drops to below 90 % of nominal voltage for a period exceeding 100 ms to ensure the power quality and avoid unbalances. However, this rule shows that the generators will often cut out of the network whenever a fault happens near the connection node. Results in the figures from Fig. 12 to Fig. 15 showed a forecast result in voltage instability of node and the operator can adjust the parameters of relays again and set the operating mode of network in a reasonable manner.

The simulation results from Fig. 12 to Fig. 15 are calculated in a natural state operation and the operation of protective relay systems is not considered.

V. CONCLUSIONS

The distribution network connected wind turbine (induction machine type) has many potential factors affecting on the voltage quality, including the risk of voltage instability. Therefore, the consideration of voltage stability limits when operating the distribution network connected induction machine is an imperative content. The connecting node with this machine type should be considered first priority because of the most loss of voltage [1], [3]. The limits on the voltage and power should be interested in improvement.

DFIM generators can produce reactive power, so most distribution networks with DFIM may not need to install compensated equipment. The distribution network with DFIM gives voltage quality better than IM.

PV characteristic of DFIM has the stability area extension better than IM. When considering node voltage decline, the ability to stabilize the voltage of DFIM is better than IM.

Through the expressions (17) to (20) also showed that, in order to improve stability, the ratio X/R and short-circuit power of the system have an important significance. Due to the system impedance calculated by short-circuit power SN, so the larger value of SN the stability limit is better, while also reduces the probability of shutdown generator due to voltage drops in neighbouring area with nodes connected wind generators.

REFERENCES

- [1] J. V. Milanovic, T. M. David, "Stability of distribution networks with embedded generators and induction motors", in *IEEE PES Winter Meeting*, 2002, vol. 2, pp.1023–1028.
- [2] P. Aree, "Load flow solution with induction motor", *Songklanakarin J. Sci. Technol.*, vol. 28, no. 1, pp. 157–168, 2006.
- [3] V. Rimas, M. Shinozuka, M. Takeno, "Parameters study of wind loading on structures", *Journal of the Structural Div., ASCE*, 1973, pp. 453–468.
- [4] T. T. Chuong, "Voltage stability investigation of network connected wind farm", in *Proc. World Academy of Science, Engineering and Technology*, vol. 32, 2008.
- [5] J. G. Sloopweg, "Modelling and impact on power system dynamics", Ph.D. dissertation, University Delft, 2003.
- [6] J. O. Tande, "Applying power quality characteristics of WTs for assessing impact on voltage quality", *Wind Energy*, vol. 5, no. 1, pp. 37–52, 2002. [Online]. Available: <http://dx.doi.org/10.1002/we.59>
- [7] S. Kelouwani, K. Agbossou, "Nonlinear model identification of WT with a neural network", in *IEEE Trans. on Energy Conversion*, vol. 19, no. 3, 2004.
- [8] J. Vu, V. T. Soens, P. Driesen, R. Belmans, "Modeling WT generators for power system simulations", in *European Wind Energy Conf. (EWEC 2003)*, Madrid, 2003, pp. 16–19.
- [9] S. Repo, H. Laaksonen, P. Jarventausta, O. Huhtala, M. Mickelsson, "A case study of a voltage rise problem due to a large amount of distributed generation on a weak distribution network", in *IEEE Power Tech Conf. Proc.*, Bologna, 2003, vol. 4.